Design Study of a 630-GHz Injection-Locked Oscillator Based on InP HBT Technology

Giyeong Nam and Jae-Sung Rieh[a]
Department of Electrical Engineering, Korea University
E-mail : [a]jsrieh@korea.ac.kr

***Abstract* – In this work, an injection-locked oscillator (ILO) has been designed in a 250-nm InP HBT technology for operation around 630 GHz. The ILO is based on LC cross-coupled topology with push-push structure for second harmonic extraction and fundamental signal suppression. The on-chip patch antenna is integrated to the output stage of the ILO for direct radiation into free space. The injection circuit is formed at the emitter stage of the ILO with transformer based passive balun for compact design. It will also suppress the loss that can be induced by an active circuit in the high-frequency band. The delivered output power in free-running condition is -7.6 dBm at 637.3 GHz. With an injection signal of 0 dBm at 320 GHz, the delivered output power is 1 dBm at 640 GHz. The total DC power consumption is 20.6 mW.**

***Keywords*—Injection locked oscillator, patch antenna, 250-nm InP HBT**

I. INTRODUCTION

The terahertz (THz) band generally refers to the frequency range from 0.1 to 10 THz. It corresponds to wavelengths of approximately 0.03–3 mm, partially encompassing the sub-millimeter-wave (sub-mm) region with wavelengths below 1 mm. Owing to the much higher carrier frequency than conventionally employed bands, substantially wider bandwidths and higher data-throughput can be achieved. Historically, applications in this band —positioned between the optical and electronic domains— have been led by optics-based applications such as spectroscopy and imaging. Recently, however, rapid advances in the performance of electronic devices have invigorated research based on electronic approaches, including communication and radar systems [1].

For semiconductor–based systems, reliable on-chip THz signal sources are highly desirable. Two widely adopted approaches to implement such sources are on-chip oscillators and frequency multipliers. THz on-chip oscillators can operate without an external reference but, as with voltage-controlled oscillators (VCOs), may suffer from limited tuning range and output-amplitude variation. By contrast, frequency multipliers can realize wider operational bandwidths with relatively small amplitude variation. However, when used alone, their output power is often limited and their phase-noise performance is degraded (e.g., scaling with the multiplication factor) [2]. To overcome this limitation and enable operation at high frequencies, injection-locked oscillators (ILOs) are widely employed [3]. A conceptual comparison of the phase-noise characteristics of an oscillator, a frequency multiplier (FM), and an ILO is depicted in Fig. 1. The objective of this work is to design an ILO operating around 630 GHz that achieves both high output power and wide operational bandwidth, performance metrics that are crucial for THz systems.

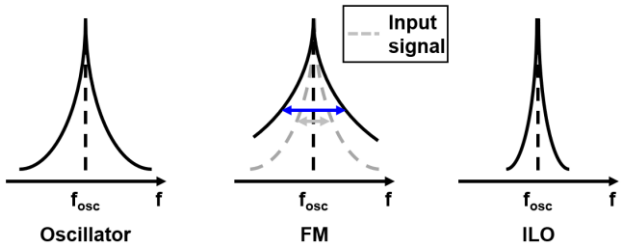

Fig. 1. Conceptual comparison of the phase-noise characteristics of (a) oscillator, (b) FM and (c) ILO.

Architectures of injection-locked oscillators (ILOs) can be classified by the oscillator topologies and the injection methods. In [4], [5], injection is applied at the base of one transistor in a ring oscillator. These approaches achieve good performance at very high frequencies, but at the cost of high circuit complexity and elevated DC power consumption. In [6], [7], LC cross-coupled oscillators are used. In this case, injection is realized either by adding a transistor in parallel with the oscillator core or by magnetic coupling through a transformer, both demonstrating good performance. However, transformers and extra transistors may exhibit significant loss above 300 GHz, making them difficult to employ. Therefore, in this work, we adopted an LC cross-coupled oscillator to reduce complexity and to facilitate a push–push configuration, and we implemented the injection path as a passive network to avoid high-frequency loss,

a. Corresponding author; jsrieh@korea.ac.kr

Manuscript Received Sep. 5, 2025, Revised Dec. 8, 2025, Accepted Dec. 24, 2025

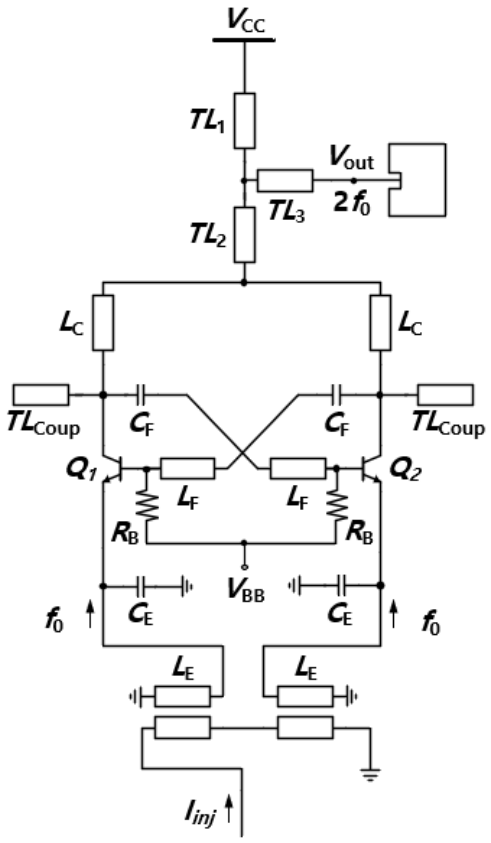

Fig. 2. Circuit schematic of the proposed ILO.

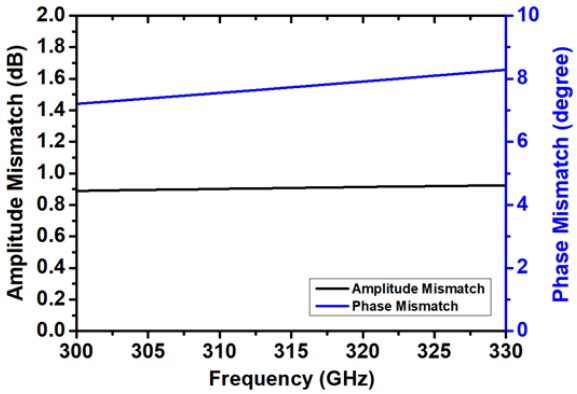

(a)

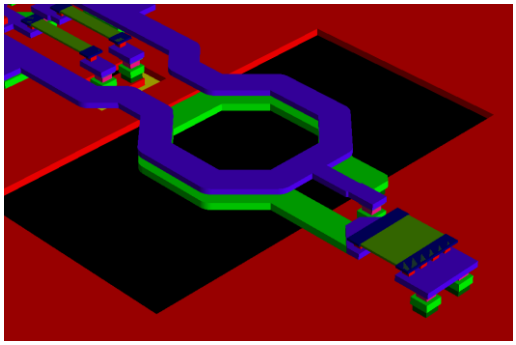

(b)

Fig. 3. (a) Simulated results and (b) 3-D view of transformer-based balun.

thereby realizing an injection-locked oscillator. In Section II, designed 637-GHz ILO is described with details. The simulated results of ILO are shown in Section III. Lastly, the conclusion is presented in Section IV.

II. 637-GHZ INJECTION-LOCKED OSCILLATOR

The proposed ILO shown in Fig. 2 is based on LC cross-coupled topology with a push-push structure for second harmonic extraction and fundamental signal suppression. The mid-size transistors ($A_E = 5 \times 0.25\,\mu m^2$) have been adopted for Q_1 and Q_2 to satisfy the output power requirement and ensure stable fundamental oscillation around 300 GHz. To achieve a lower admittance, a capacitive degeneration is adopted for the emitter stage of the oscillator core [8]. To implement capacitive degeneration at the emitter stage, a transmission-line based RF choke or short stub must be connected in parallel with the degeneration capacitor to provide a DC current path and inductance. For implementing the ILO, it is essential to provide an external signal-injection point. In the proposed circuit, a transformer-based balun is inserted at the emitter node to implement the injection path. Leveraging the balun allows the emitter inductor to be implemented within the balun itself, eliminating the need for additional shunt transmission lines and thereby improving area efficiency. Moreover, the balun converts the single-ended input into a differential signal, enabling injection into each transistor of the push–push oscillator's differential core, so that the injected signal is properly processed within the core. The amplitude and phase balance of the transformer-based balun are depicted in Fig. 3(a), and Fig. 3(b) shows the 3-D layout views of each. The amplitude and phase mismatch of the balun at the designed oscillation frequency of the oscillator show about 0.9 dB and 7.5˚, respectively. The insertion loss of the balun is about 3.8 dB at the designed oscillation frequency, which incorporates the 3-dB degradation associated with the conversion from single-ended to differential operation. When compared with the case without

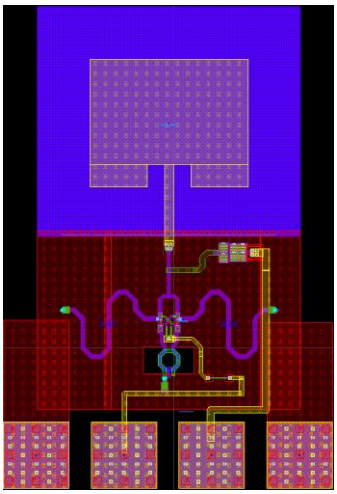

Fig. 4. Layout of the proposed ILO.

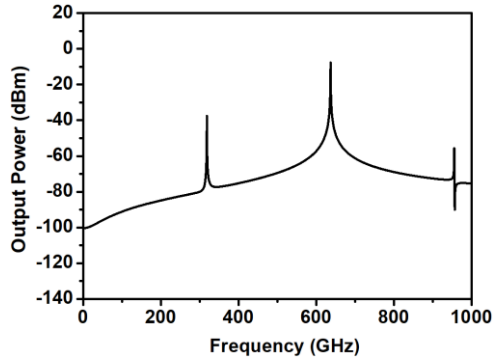

(a)

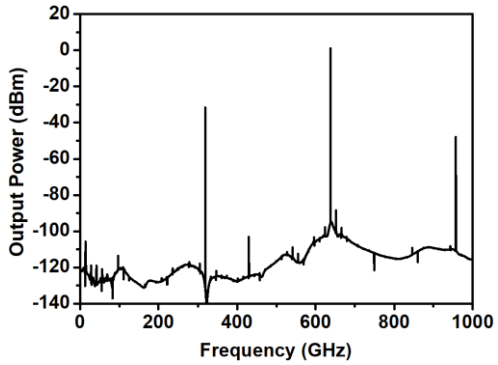

(b)

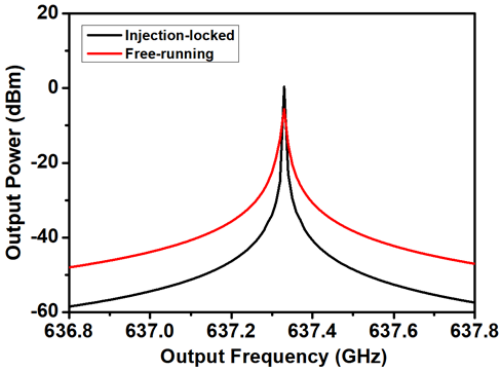

(c)

Fig. 5. Simulated results of the ILO: (a) Output spectrum of free-running condition and (b) Output spectrum of injected condition and (c) Spectrum comparison between free-running and injected condition at the free-running frequency.

a mismatch, the input transformer based balun exhibited a 0.7˚ improvement in the differential phase imbalance between the collector nodes of the oscillator core under free-running oscillation, leading to a 2.8-dB enhancement in the second-harmonic output power. In addition, when a 0-dBm external injection signal was applied, the phase difference and the output power improved by 0.1˚ and 0.3 dB, respectively. However, in the actual layout, s mismatch was induced in the balun to satisfy the design-rule constraints, resulting in the behavior shown in Fig. 3(a).

For the direct radiation of the generated 637-GHz signal into the free space, an on-chip patch antenna was integrated. Implementing a patch antenna enables spatial combining, which offers better scalability than employing an on-chip power combining circuit. On-chip power combining not only

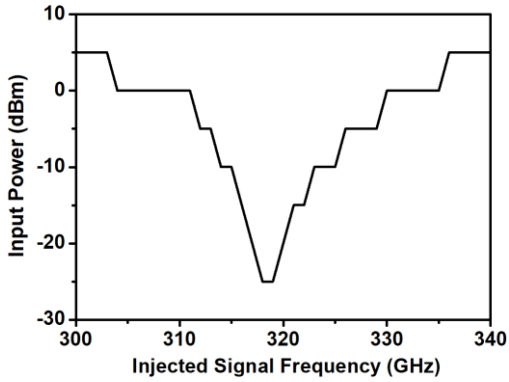

Fig. 6. Simulated result of sensitivity

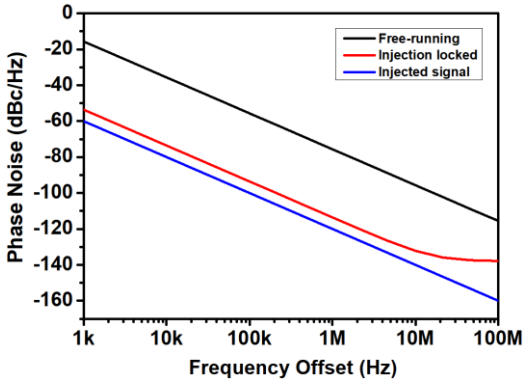

Fig. 7. Simulated phase noises for the free running condition and the injected condition.

complicates the layout when realizing a 2-D array, but also introduces additional loss in the power-combining network at high frequencies. Accordingly, using an on-chip antenna with spatial combining can provide a larger increase in effective isotropic radiated power (EIRP) for array implementations than the approach based on on-chip power combining. The EIRP expression of N × N array is given by:

$$\text{EIRP} = P_{rad,unit} \times G_{unit} \times N^4 \qquad (1)$$

where $P_{rad,unit}$ is the radiated power of unit oscillator and G_{unit} is the antenna gain of unit oscillator. As indicated by (1), when spatial combining is employed, EIRP scales quadratically with the number of unit oscillators in the array. According to the antenna array simulations, increasing the array size to four elements results in an approximately 5-dB increase in directivity, while the half-power beam width (HPBW) decreases to about one-third of that of a single element. This is significantly narrower compared to the single-element case. This trade-off arises because, as the number of array elements increases, spatial combining concentrates the radiated power more strongly in a specific direction, thereby increasing the directivity and correspondingly reducing the HPBW.

The TL_{coup} depicted in the schematic of Fig. 2 denotes the coupling transmission line that connects each oscillator to its two nearest neighbors in the array to realize inter–injection locking. The length of TL_{coup} is set to λ/2 at the fundamental

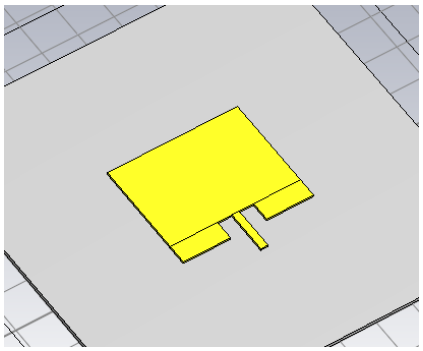

(a)

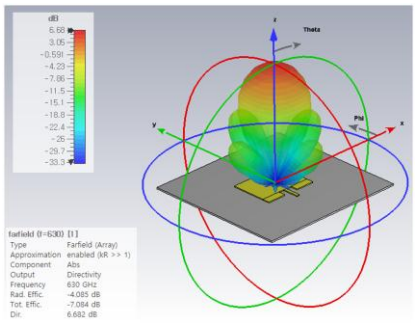

(b)

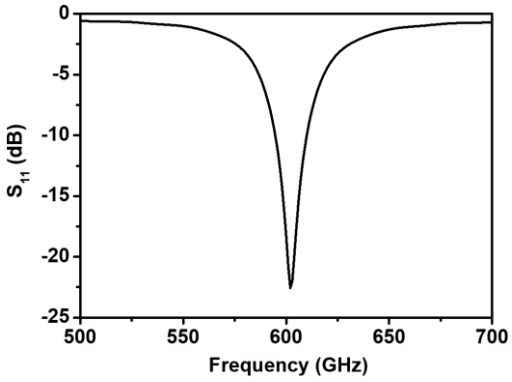

(c)

Fig. 8. (a) 3-D view, (b) far-field and (c) S-parameter simulation result of integrated patch antenna

oscillation frequency. Under in-phase coupling, the midpoint between the two coupled TLs becomes a virtual open circuit. Since each TL_{coup} is λ/2 at the fundamental frequency, the impedance seen from the oscillator core looking into the TL_{coup} is transformed to an open, thereby imposing negligible loading on the oscillator core.

While vertical coupling is not employed in this design, it can be incorporated in future work to realize a 2-D array. Several topologies can be used to implement the vertical coupling, such as meander-line and ring-type structures. More specifically, these structures can be realized by connecting the oscillators located at both ends of each horizontal coupling row to the corresponding oscillators in the upper and lower rows.

TABLE I. Comparison of Oscillators Near 600 GHz

Ref.	Tech.	# of Power Comb.	Freq (GHz)	P_{rad} (dBm)	P_{rad} per unit (dBm)	Phase Noise @ 1 MHz Δf (dBc/Hz)	Area (mm^2)
[9]	65-nm CMOS	32	679.4-716.1	-2.4	-17.4	-72.1	0.97
[10]	40-nm CMOS	8	660.8-676.6	-16.1	-16.1	-69	0.86
[11]	40-nm CMOS	36	584-590	0. 1	-15.5	-82	0.68
[12]	250-nm InP HBT	1	556-610	-11.2*	-11.2*	-	0.11
[13]	250-nm InP HBT	1	560-645	-17.4*	-17.4*	-	0.14
[14]	250-nm InP HBT	1	573.1	-19.2*	-19.2*	-	0.41
[8]	250-nm InP HBT	1	580-586	-7.5	-7.5	-88.6	0.29
[15]	130-nm InP HBT	1	698.8-702.3	-11.8	-11.8	-73.8	0.41
This work	250-nm InP HBT	1	637.3	-11.7	-11.7	-75.7[a] / -113.6[b]	0.18

*Output power measured with probes
[a]free-running condition
[b]external signal source injected with -120 dBc/Hz @ 1-MHz offset

III. SIMULATION RESULTS AND DISCUSSION

The simulations were performed in ADS (Advanced Design System) using the transient simulation, the harmonic-balance technique, and full-wave EM analysis with ADS Momentum. Fig. 4 shows the layout of the developed ILO. The chip size is $374 \times 548\ \mu m^2$ and DC power consumption is 20.6 mW. Fig. 5 presents the oscillator output spectra, which were obtained by applying a fast Fourier transform (FFT) to the transient simulation results. In the free-running condition, the delivered output power—defined as the power delivered to the on-chip patch antenna—is −7.6 dBm at 637.3 GHz, as shown in Fig. 5(a). Fig. 5(b) shows the delivered output power under injection. When a 0-dBm external signal at 320 GHz is applied, the delivered output power is 1 dBm at 640 GHz. Fig. 5(c) compares the output spectrum under free-running and injection-locked conditions, which correspond to the cases shown in Fig. 5(a) and (b), respectively. Compared with the free-running case, the injection-locked spectrum exhibits a narrower spectrum profile with a higher peak output power, consistent with the conceptual illustration in Fig. 1 in Section I. The sensitivity curve in Fig. 6, which was obtained with the input power stepped at 5-dB increments, indicates that injection locking is achieved with an injected signal frequency over 304–335 GHz when assuming the an injection signal of 0 dBm.

Fig. 7 plots the simulated phase-noise (PN) of the ILO. The PN is simulated by the PN setup which includes the harmonic-balance noise controller and a PN source. Under the free-running condition (no external injection), the oscillator exhibits −75.7 dBc/Hz at a 1-MHz offset. To obtain the phase noise for the injected case, an external source with a phase noise of −120 dBc/Hz at a 1-MHz offset was assumed near the injection frequency around 300 GHz, which is a realistic noise level typically available with commercial signal sources (Anritsu MG36241A). With the proposed ILO employing a push–push architecture that extracts the second harmonic, the ideal phase noise level would be around 6 dB higher than the injected noise, or −120 dBc/Hz at a 1-MHz offset at the second harmonic. The ILO

exhibited a phase noise of −113.6 dBc/Hz at a 1-MHz offset by simulation, which is consistent with the expected value. In a complete system, the attainable output phase noise will be limited by the phase noise of the injection source, yet it remains substantially better than the free-running case. Moreover, when extended to an oscillator array, inter-injection locking among adjacent oscillators can further reduce the phase noise [16].

Fig. 8 shows a 3-D view of the patch antenna which is integrated at the output node of the ILO, and the corresponding far-field and S-parameter simulation results. The simulations were performed using CST. The antenna exhibits a directivity of 6.2 dB and a radiation efficiency of −3.9 dB, resulting in an antenna gain of 2.3 dB. The S-parameter simulation results are shown in Fig. 8(c). The patch antenna was designed for 600 GHz — slightly lower than the intended oscillation frequency — to accommodate an expected process-induced frequency down-shift of up to about 5% in the fabricated circuit. This value is estimated based on the results of other oscillators fabricated using the same process within our group. Consequently, the measured radiation efficiency may improve, and the antenna gain may increase accordingly. The simulated total efficiency, which includes radiation efficiency and insertion loss, at 600 GHz is slightly improved, showing a 2.3-dB increase compared to the simulated result at 630 GHz.

Table I compares the oscillator presented in this work with previously reported oscillators operating near 600 GHz. Although some prior works employed array configurations to increase the output power, this work focuses on a single-element oscillator and demonstrates its potential scalability toward array implementations. When the radiated output power is normalized on a per-element basis, the proposed oscillator exhibits competitive performance relative to existing designs. In terms of phase-noise performance, the proposed design shows comparable characteristics under free-running operation, while achieving superior phase-noise performance with injection-locking by an external signal source.

IV. CONCLUSION

A 630-GHz injection-locked oscillator (ILO), which comprises an injection port and an integrated on-chip patch antenna, has been successfully designed based on 250-nm InP HBT technology. The designed circuit exhibited an output power of -7.6 dBm at 637.3 GHz with free-running oscillation condition, and an output power of 1 dBm at 640 GHz with injected signal of 0 dBm at 320 GHz. The developed ILO is expected to be well suited for various applications that require high power and wideband near 600 GHz and is planned to be measured to validate the performance. The designed ILO can be easily extended to an array in system implementations to achieve higher EIRP performance.

ACKNOWLEDGMENT

The chip fabrication and EDA tool were supported by the IC Design Education Center (IDEC), Korea.

REFERENCES

[1] J.-S. Rieh, *Introduction to Terahertz Electronics*. Springer Nature, 2021.

[2] S. Jung, J. Yun, and J.-S. Rieh, "A D-band integrated signal source based on SiGe 0.18 μm BiCMOS technology," *Journal of Electromagnetic Engineering and Science*, vol. 15, no. 4, pp. 232-238, 2015.

[3] B. Razavi, "A study of injection locking and pulling in oscillators," *IEEE journal of solid-state circuits*, vol. 39, no. 9, pp. 1415-1424, 2004.

[4] A. Siligaris *et al.*, "A 270-to-300 GHz sub-harmonic injection locked oscillator for frequency synthesis in sub-mmW systems," *IEEE Microwave and Wireless Components Letters*, vol. 25, no. 4, pp. 259-261, 2015.

[5] T. Chi, J. Luo, S. Hu, and H. Wang, "A multi-phase sub-harmonic injection locking technique for bandwidth extension in silicon-based THz signal generation," *IEEE Journal of Solid-State Circuits*, vol. 50, no. 8, pp. 1861-1873, 2015.

[6] L. Iotti, G. LaCaille, and A. M. Niknejad, "A dual-injection technique for mm-wave injection-locked frequency multipliers," *IEEE Transactions on Microwave Theory and Techniques*, vol. 69, no. 12, pp. 5417-5428, 2021.

[7] S. P. Sah and D. Heo, "An 8 th sub-harmonic injection locked V-band VCO for low power LO routing in mm-wave beamformers," in *2014 IEEE Radio Frequency Integrated Circuits Symposium*, 2014: IEEE, pp. 177-180.

[8] H. Son, J. Kim, K. Song, D. Kim, J. Yoo, and J.-S. Rieh, "600-GHz high-power signal sources based on 250-nm InP HBT technology," *IEEE Transactions on Terahertz Science and Technology*, vol. 12, no. 6, pp. 648-657, 2022.

[9] L. Gao and C. H. Chan, "A 0.68–0.72-THz 2-D scalable radiator array with–3-dBm radiated power and 27.3-dBm EIRP in 65-nm CMOS," *IEEE Journal of Solid-State Circuits*, vol. 57, no. 10, pp. 3114-3124, 2022.

[10] G. Guimarães and P. Reynaert, "A 670-GHz 4× 2 oscillator–radiator array achieving 7.4-dBm EIRP in 40-nm CMOS," *IEEE Journal of Solid-State Circuits*, vol. 56, no. 11, pp. 3399-3411, 2021.

[11] K. Guo and P. Reynaert, "29.2 A 0.59 THz beam-steerable coherent radiator array with 1mW radiated power and 24.1 dBm EIRP in 40nm CMOS," in *2020 IEEE International Solid-State Circuits Conference-(ISSCC)*, 2020: IEEE, pp. 442-444.

[12] J. Kim *et al.*, "Terahertz signal source and receiver operating near 600 GHz and their 3-D imaging application," *IEEE Transactions on Microwave Theory and Techniques*, vol. 69, no. 5, pp. 2762-2775, 2021.

[13] J. Yun, J. Kim, D. Yoon, and J. S. Rieh, "645 - GHz InP heterojunction bipolar transistor harmonic oscillator," *Electronics Letters*, vol. 53, no. 22, pp. 1475-1477, 2017.
[14] M. Seo *et al.*, "InP HBT IC technology for terahertz frequencies: Fundamental oscillators up to 0.57 THz," *IEEE Journal of Solid-State Circuits*, vol. 46, no. 10, pp. 2203-2214, 2011.
[15] H. Son, J. Yoo, D. Kim, and J.-S. Rieh, "A 700-GHz Integrated Signal Source Based on 130-nm InP HBT Technology," *IEEE Transactions on Terahertz Science and Technology*, 2023.
[16] L. Gao and C. H. Chan, "A 144-Element beam-steerable source array with 9.1-dBm radiated power and 30.8-dBm lensless EIPR at 675 GHz," *IEEE Journal of Solid-State Circuits*, vol. 59, no. 2, pp. 375-387, 2023.

Giyeong Nam received the B.S. and in electrical engineering from Dongguk University, Seoul, Korea, in 2023. He is currently pursuing the Ph.D. degree in electrical and electronics engineering from Korea University, Seoul, South Korea. His research interest includes THz signal sources and oscillators.

Jae-Sung Rieh received the B.S. and M.S. degrees in electronics engineering from Seoul National University, Seoul, Korea, in 1991 and 1995, respectively, and the Ph.D. degree in electrical engineering from the University of Michigan, Ann Arbor, MI, USA, in 1999. In 1999, he joined IBM Semiconductor R & D Center, where he was responsible for the development of high frequency SiGe HBT technologies. Since 2004, he has been with the School of Electrical Engineering, Korea University, Seoul, Korea, where he is currently a Professor. Prof. Rieh was a recipient of IBM Faculty Award (2004) and a co-recipient of IEEE EDS George E. Smith Awards (2002 and 2006) and IEEE Microwave and Wireless Component Letters Tatsuo Itoh Best Paper Award (2013). He has served as an Associate Editor of the IEEE Microwave and Wireless Components Letters (2006-2009) and the IEEE Transactions on Microwave Theory and Techniques (2010-2013). In 2012 and 2018, he was a visiting scholar at Submillimeter Wave Advanced Technology team (SWAT) in JPL, Pasadena, USA, and at High Speed Electronics Lab (HSEL) in UCLA, Los Angeles, USA, respectively. He is the author of the book, “Introduction to Terahertz Electronics (Springer, 2021)”. His major research interest lies in the mm-wave and terahertz devices and circuits.